# PERFORMANCE OF A SOLAR-BIOMASS POWERED THERMODYNAMIC CYCLE INCORPORATING THE HYGROSCOPIC CYCLE TECHNOLOGY (HCT)

Andrés Meana-Fernández[1]*, Roberto Martínez-Pérez[1], Francisco J. Rubio-Serrano[2], Antonio J. Gutiérrez-Trashorras[1]

[1]University of Oviedo, Thermal Machines and Engines Area, Department of Energy, C/Wifredo Ricart, s/n 33204 Gijón, Spain

[2]IMATECH, IMASA Technologies, S.L.U. C/Carpinteros 12, 28670 Villaviciosa de Odón, Madrid, Spain

*Corresponding Author: andresmf@uniovi.es

## ABSTRACT

Climate change challenges translate into higher ambient temperatures, as well as other problematics as freshwater depletion. In this context, power generation systems based on solar energy represent a solution to establish a sustainable generation system in terms of pollutants emissions. In this work, the performance of a solar-biomass powered thermodynamic cycle incorporating the Hygroscopic Cycle Technology (HCT) to reduce climate change hazards is evaluated. Condensation within the cycle takes place in an absorber, utilizing water solutions of hygroscopic compounds, resulting in higher condensing temperatures with respect to traditional steam cycles. This allows using dry coolers at places with high ambient temperatures, eliminating completely the need for cooling water. Considering the vulnerability of Mediterranean regions to climate change effects, a case study for a 12.5 MW biomass cycle in Córdoba (southern Spain) is presented, evaluating its energy and exergy efficiency through thermodynamic models developed with Engineering Equation Solver. Afterwards, a sensitivity analysis has been performed to assess the effect of solar integration and ambient temperatures on the system. Additionally, the reduction in direct carbon emissions due to the introduction of solar energy is evaluated. Effective operation of the cycle up to 50ºC ambient temperature has been observed, with 32.21 energy and 25.43% exergy efficiency values at the design point (35ºC). Integration of 5 MW of solar thermal power was found to increase exergy efficiency by around 1.7%, avoiding the emission of 16.637 tons of $CO_2$ and 25.4 kg of $SO_2$ per day. The results hint at a positive local impact in the region of Córdoba in terms of the efficiency of the cycle and its environmental impact; in addition, they may be extrapolated to other Mediterranean locations with similar climate conditions. As regions with water scarcity and high ambient temperatures tend to have high solar irradiation values, solar-HCT may represent an advantage with respect to traditional systems.

## 1 INTRODUCTION

Global electricity demand is expected to rise from its current level by over 80% to more than 150% by 2050 (IEA, 2023), with fossil fuel consumption reaching a peak by 2023 and then declining sharply. The additional demand, bound to happen for all the considered scenarios, will be met by low-emission sources, such as renewables, nuclear power, fossil fuels equipped with carbon capture, and hydrogen and ammonia as energy vectors. Only with this type of strategies will it be possible to reach the Net Zero Emissions scenario by 2050 and keep the 1.5ºC goal in reach. The United Nations World Water Development Report (United Nations, 2023) sets a more problematic scenario for 2050, with increasing water demand. Global urban population facing water scarcity is projected to rise from 930 million in 2016 to 1.7–2.4 billion people in 2050 (He et al., 2021). In these scenarios of water scarcity and rising ambient temperatures, power generation technologies requiring heat dissipation to the environment are going to face challenges for continuing their operation, with resource stress affecting energy security (Axon and Darton, 2021) These challenges require bold technical improvements in thermodynamic



https://doi.org/10.52202/077185-0012

power systems to guarantee energy supply. Due to the intermittency of most of renewable energy technologies, many solutions rely in the coupling of these technologies, such as solar power (Zhang et al, 2022) or geothermal resources (Nsanzubuhoro et al., 2020), with conventional ones. Interest has been set as well in combined heat and power cycles, capable of supplying heat and power simultaneously. Again, examples may be found in the analysis of solar (Suárez-López et al., 2020) and geothermal (Fiaschi et al., 2021) systems.

In the context of water scarcity and rising ambient temperatures, the Hygroscopic Cycle Technology (HCT), developed by IMASA Technologies, S.L.U. (Rubio-Serrano et al., 2018), represents a feasible solution based on mixtures of water and hygroscopic compounds that allows condensation of the turbine exhaust steam through its absorption. This technology allows rejecting heat without the use of an auxiliary cooling water circuit, with dry coolers used to extract heat directly from the working fluid. Consequently, the gap between cycle operating temperatures and ambient temperature may be narrower than in other power generation technologies. In addition, hygroscopic effects result in higher condensing temperatures for a given pressure with respect to traditional steam cycles. When implemented in the Vetejar (Córdoba, Spain) 12.5 MW biomass power plant, property of an olive oil industry, energy availability was extended by an average of 75 MWh/month, cutting all cooling water needs (229,200 $m^3$/year). This biomass power plant is powered burning orujillo, a byproduct of olive oil production, with no additional cost to the company.

With the focus set in improving the cycle efficiency, reaching a better heat utilization, and reducing the emissions generated by burning orujillo, in this work, the hybridization of the biomass boiler with a solar field is considered. The reason is that the challenges in water scarcity and rising ambient temperatures are expected to be harder in regions with available solar resources. Considering the particular vulnerability of Mediterranean regions to the effects of climate change, a case study is presented for Córdoba, located in southern Spain. The energy and exergy efficiency of the facility will be evaluated, and an estimation of avoided emissions will be provided.

## 2 MATERIALS AND METHODS

A case study based on the operating conditions of Vetejar (Córdoba, Spain), which runs on orujillo biomass obtained as a byproduct of olive oil production, will be performed by incorporating a solar field coupled in parallel with the evaporator of the biomass boiler. A thermodynamic model has been developed by applying mass and energy balances to the different cycle equipment, allowing to calculate the necessary cycle parameters and the energy efficiency. The exergy efficiency of the cycle has been assessed as well, calculating exergy destructions at the relevant equipment. Finally, a rough estimation of the avoided emissions from burning the biomass is given.

### 2.1 Case study: 12.5 MW hybrid biomass-solar power plant

The 12.5 MW Vetejar power plant has been taken as a reference and a solar field has been coupled to the steam drum of the boiler, allowing to divert part of the liquid to be evaporated and reducing the amount of biomass to be burnt. Figure 1 shows the scheme of the proposed cycle configuration, with Parabolic Trough Collectors (PTC) used for Direct Steam Generation (DSG). The live steam goes to the turbine (point 1), where part of the steam is bled (2) before the final expansion (3). Then, the exhaust steam is driven to the key component of the cycle, where is becomes absorbed by the cooling reflux (18) and finally condensed. The condensate (4) is pumped back to the bleeding pressure (5), where part of it is diverted (16) towards the cooling reflux while the rest is driven to an enthalpic recuperator (6). At this recuperator, energy from the boiler purges (14) is recovered (7). Then, the boiler purges (15) proceed to join the cooling reflux, while the feedwater is heated up in a deaerator with the turbine bleeding (2). Afterwards, the feedwater (8) is pumped to the boiler pressure (9), passing across the economizer and reaching liquid state (10). This saturated liquid is driven to the steam drum, where it is directed either to the biomass boiler evaporator (11) or to the solar field (19), coming back as saturated steam (12 and 20). Finally, the saturated steam goes to the boiler superheater (13), reaching live steam conditions (1).


https://doi.org/10.52202/077185-0012

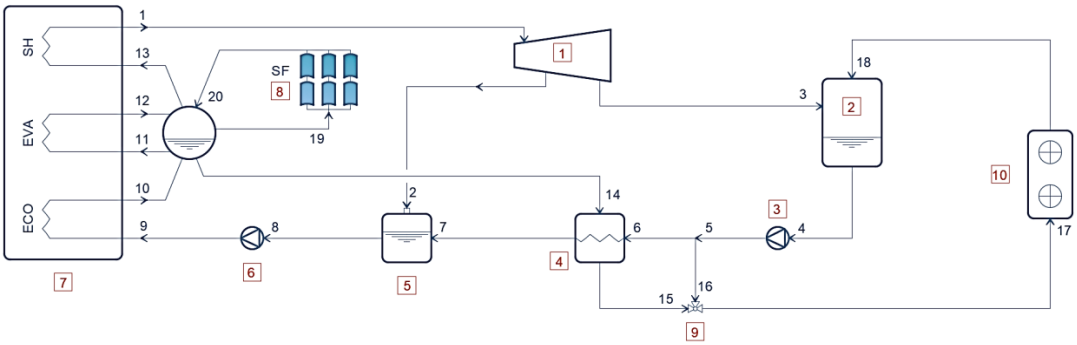


**Figure 1:** Scheme of the proposed cycle configuration.

The operating conditions used to generate the thermodynamic model are collected in Table 1. The absorber pressure was modified as a function of the cooling reflux temperature to control the temperature drop in the dry coolers and the approach point with ambient temperature, to keep the net power of the cycle as stable as possible. Different values of ambient temperatures and solar thermal power integration into the cycle have been studied to consider their effects on cycle performance.

**Table 1:** Thermodynamic conditions of the cycle.

| Variable | Value | Units |
|---|---|---|
| Boiler pressure | 80 | bar |
| Live steam temperature | 480 | ºC |
| Bleeding pressure | 2 | bar |
| Absorber pressure | 0.05-0.30 | bar |
| Approach point at enthalpic recuperator | 5 | ºC |
| Turbine isentropic efficiency | 80% | - |
| Isentropic efficiency of pumps | 85% | - |
| Boiler efficiency | 87% | - |
| Turbine power | 12.5 | MW |

### 2.2 Thermodynamic model: energy and exergy analyses

For developing the thermodynamic model, steady operating conditions have been considered. As the concentration of hygroscopic compounds found in industrial applications of the cycle is low enough (below 0.01%), thermodynamic properties of all cycle streams may be approximated with those of pure water with negligible error. In this work, focus has been set on the thermodynamic cycle itself (i.e., electric power consumption at dry coolers and modelling of biomass combustion are not considered). The change in kinetic and potential energy, as well as pressure and heat losses have been neglected too. With all these assumptions, mass and energy balances following Equations 1 and 2 have been performed at all the relevant equipment, using Engineering Equation Solver (F-Chart Software, 2024):

$$\sum_{in} \dot{m}_i = \sum_{out} \dot{m}_i \tag{1}$$

$$\dot{Q} - \dot{W} + \sum_{in} \dot{m}_i \, h_i - \sum_{out} \dot{m}_i \, h_i = 0 \tag{2}$$

where $\dot{m}_i$ represent all the relevant mass flowrates in kg/s, $\dot{Q}$ is the heat transfer rate in kW, $\dot{W}$ is the power in kW, and $h_i$ are the relevant enthalpy values in kJ/kg. The power produced by the turbine is:

$$\dot{W}_T = \dot{m}_1 \cdot (h_1 - h_2) + \dot{m}_3 \cdot (h_2 - h_3) \tag{3}$$

The power consumption at the condensate and feeding pumps is:



https://doi.org/10.52202/077185-0012

$$\dot{W}_{CP} = \dot{m}_4 \cdot (h_5 - h_4) \quad (4)$$

$$\dot{W}_{FP} = \dot{m}_4 \cdot (h_9 - h_8) \quad (5)$$

The thermal power required at the economizer is:

$$\dot{Q}_{ECO} = \dot{m}_9 \cdot (h_{10} - h_9) \quad (6)$$

whereas, for evaporation, it is:

$$\dot{Q}_{EVA} = \dot{m}_{13} \cdot h_{13} - \dot{m}_{10} \cdot h_{10} + \dot{m}_{14} \cdot h_{14} \quad (7)$$

and at the superheater is:

$$\dot{Q}_{SH} = \dot{m}_1 \cdot (h_1 - h_{13}) \quad (8)$$

So, the total thermal power input is:

$$\dot{Q}_{in} = \dot{Q}_{ECO} + \dot{Q}_{EVA} + \dot{Q}_{SH} \quad (9)$$

This heating power is provided by the biomass boiler and the solar field:

$$\dot{Q}_{in} = \dot{Q}_{BIO} + \dot{Q}_{SOLAR} \quad (10)$$

Hence, the amount of biomass to be burnt may be obtained as:

$$\dot{m}_{BIO} = \frac{\dot{Q}_{BIO}}{LHV_{BIO} \cdot \eta_b} \quad (11)$$

where $LHV_{BIO} = 18246.42$ kJ/kg, the value for orujillo (ANEO, 2024) and $\eta_b$, the boiler efficiency, has been set to 87%, in line with values for fluidized bed combustion boilers (Ke et al., 2022).

On the other hand, the heat dissipation requirements at the dry cooler may be calculated as:

$$\dot{Q}_{DC} = \dot{m}_{17} \cdot (h_{17} - h_{18}) \quad (12)$$

Finally, the cycle efficiency may be obtained as the ratio between the net power and the thermal power input required:

$$\eta_I = \frac{\dot{W}_{net}}{\dot{Q}_{in}} = \frac{\dot{W}_T - \dot{W}_{CP} - \dot{W}_{FP}}{\dot{Q}_{in}} \quad (13)$$

The exergy efficiency of the cycle has been calculated by obtaining the different exergy values of the streams and calculating exergy destructions and losses at all the relevant equipment. For this first approximation, only physical exergy has been considered, as the differences in hygroscopic compound concentrations between the different stream flow may be neglected. Therefore, the exergy of each stream is:

$$\dot{E}x_i = \dot{m}_i[(h_i - h_0) - T_0 \cdot (s_i - s_0)] \quad (14)$$

where $T_0$ is the ambient temperature in K, $h_0$ and $s_0$ are the enthalpy and entropy of water at ambient temperature in kJ/kg and kJ/(kg·K) respectively, and $s_i$ is the entropy of each stream in kJ/(kg·K). The chemical exergy of the biomass to be burnt may be calculated as:


https://doi.org/10.52202/077185-0012

$$\dot{E}x_{BIO} = \beta_{BIO} \cdot LHV_{BIO} \tag{15}$$

where $\beta_{BIO}$ is an experimental coefficient, with a value of 1.121 for orujillo obtained from the correlation of Szargut and Stylyska (1964). On the other hand, the exergy of solar thermal power is obtained from Winter, Sizmann, and Vant-Hull (2012):

$$\dot{E}x_{SOLAR} = \dot{Q}_{SOLAR} \cdot \left[1 - \frac{4}{3}\frac{T_0}{T_{SUN}}(1 - 0.28 \ln f_{dil})\right] \tag{16}$$

where $T_{SUN}$ =5800 K is the sun surface temperature and $f_{dil}$ =1.3·10$^{-5}$ is the so-called dilution factor.

Following the specifications of Lazzaretto and Tsatsaronis (2006), a 'fuel' and 'product' are defined for each component, the product representing the desired output or effect, and the fuel representing the input required to generate this product. Their exergy values, named as $\dot{E}x_F$ and $\dot{E}x_P$ respectively, allow to obtain the exergy efficiency of each component as:

$$\varepsilon = \frac{\dot{E}x_P}{\dot{E}x_F} \tag{17}$$

Additionally, exergy destructions and losses at every component, depending on whether they are avoidable or not, may be obtained as the difference between the exergy of all inputs and outputs:

$$\left.\begin{matrix}\dot{E}x_{D_i} \\ \dot{E}x_{L_i}\end{matrix}\right\} = \dot{E}x_{in_i} - \dot{E}x_{out_i} \tag{18}$$

The exergy efficiency of the cycle may be obtained as the useful exergy output (power from the turbine) divided by the necessary exergy input (exergy of biomass, solar power and pumps), or by adding all the destructions and losses and subtracting them from the exergy input:

$$\eta_{II} = \frac{\dot{W}_T}{\dot{E}x_{BIO} + \dot{E}x_{SOLAR} + \dot{W}_{CP} + \dot{W}_{FP}} \tag{19}$$

$$\eta_{II,ind} = 1 - \frac{\sum_i (\dot{E}x_{D_i} + \dot{E}x_{L_i})}{\dot{E}x_{BIO} + \dot{E}x_{SOLAR} + \dot{W}_{CP} + \dot{W}_{FP}} \tag{20}$$

Once the model was completed, the effect of different ambient temperatures (from 5 to 50ºC) and solar thermal power values (from 0 to 5 MW) in the cycle performance were studied. A reference case for summer temperatures in Córdoba will be described in detail, showing the ability of the cycle to work effectively without the need of water consumption for cooling purposes at 35ºC ambient temperature.

### 2.3 Environmental impact estimation

Finally, an estimation of the daily avoided carbon and sulfur emissions thanks to the reduction in the amount of biomass burnt may be obtained from the following equations, considering that orujillo has 50.02% C and 0.14% S:

$$CO_{2,avoided} = 8 \cdot 3600 \cdot 0.5002 \cdot \dot{m}_{BIO,saved} \cdot \frac{44}{12} \tag{21}$$

$$SO_{2,avoided} = 8 \cdot 3600 \cdot 0.0014 \cdot \dot{m}_{BIO,saved} \cdot \frac{64}{32} \tag{22}$$

where it has been considered that the solar field is able to work an average of 8 h/day. The final fraction in the equations comes from the stoichiometric and complete combustion equations for orujillo.



https://doi.org/10.52202/077185-0012

# 3 RESULTS AND DISCUSSION

## 3.1 Reference case: summer in Córdoba, Spain

The results obtained for the cycle thermodynamic states when considering an ambient temperature of 35ºC are collected in Table 2. It may be appreciated how, thanks to the configuration of the cycle with a condensing temperature of 53.97ºC, it is possible to reach the dry coolers at 53.99ºC, so heat release to the environment is not a problem for the hygroscopic cycle if adequate operating conditions are set. In addition, as no water is used for cooling, the configuration seems promising for regions with high ambient temperatures and water scarcity. There is, indeed, a high recirculation flow for the cooling reflux, around 416 kg/s, but it has been industrially proven that it is technically viable by Rubio-Serrano et al. (2018). Nevertheless, under the studied conditions, the power required by the condensate pump is around 94.4 kW, less than for the feedwater pump, around 133.9 kW. The net power produced by the cycle is 12.272 MW. In total, 37.975 MW of heat are absorbed from the combustion of 2.392 kg of biomass per second, resulting in a cycle energy efficiency of 32.31%.

**Table 2:** Thermodynamic states at the cycle for $T_0$=35ºC with no solar thermal power integration.

| Stream ID | $\dot{m}$ [kg/s] | P [bar] | T [ºC] | h [kJ/kg] | s [kJ/(kg·K)] |
|---|---|---|---|---|---|
| 1 | 13.24 | 80 | 480 | 3350 | 6.661 |
| 2 | 1.324 | 2 | 120.2 | 2688 | 7.082 |
| 3 | 11.92 | 0.15 | 53.97 | 2374 | 7.322 |
| 4 | 427.8 | 0.15 | 53.97 | 225.9 | 0.7549 |
| 5 | 427.8 | 2 | 53.98 | 226.2 | 0.755 |
| 6 | 12.46 | 2 | 53.98 | 226.2 | 0.755 |
| 7 | 12.46 | 2 | 65.1 | 272.7 | 0.8948 |
| 8 | 13.78 | 2 | 120.2 | 504.7 | 1.53 |
| 9 | 13.78 | 80 | 121.2 | 514.4 | 1.534 |
| 10 | 13.78 | 80 | 295 | 1317 | 3.208 |
| 11 | 13.24 | 80 | 295 | 1317 | 3.208 |
| 12 | 13.24 | 80 | 295 | 2759 | 5.745 |
| 13 | 13.24 | 80 | 295 | 2759 | 5.745 |
| 14 | 0.5452 | 80 | 295 | 1317 | 3.208 |
| 15 | 0.5452 | 80 | 58.98 | 253.6 | 0.8143 |
| 16 | 415.3 | 2 | 53.98 | 226.2 | 0.755 |
| 17 | 415.9 | 2 | 53.99 | 226.2 | 0.7551 |
| 18 | 415.9 | 2 | 39.21 | 164.4 | 0.5617 |

Considering the results from the exergy analysis, the exergy efficiency of the cycle is 25.43%. Table 3 collects the values for the exergy of fuels, products, exergy destructions, exergy losses and exergy efficiencies of the relevant cycle equipment (note that the solar field is inactive in this reference case). Figure 4 shows the contributions of cycle equipment to total exergy destruction and exergy loss. It may be observed that the biomass boiler is the component with the highest contribution to exergy destruction, with around 87.7% of the total. The second component in exergy destruction is the turbine, with around 7.1%. On the other hand, although the exergy efficiency of the absorber, the enthalpic recuperator and the dry cooler is not very high, their net contribution to destruction and losses is not so significant.

**Table 3:** Exergy analysis at $T_0$=35ºC with no solar thermal power integration.

| ID | Component | $\dot{E}x_F$ [kW] | $\dot{E}x_P$ [kW] | $\dot{E}x_D$ [kW] | $\dot{E}x_L$ [kW] | $\varepsilon$ [-] |
|---|---|---|---|---|---|---|
| 1 | Turbine | 15097 | 12500 | 2597 | 0 | 0.828 |
| 2 | Absorber | 1602 | 966.1 | 635.9 | 0 | 0.6031 |
| 3 | Condensate pump | 94.41 | 81.07 | 13.34 | 0 | 0.8587 |
| 4 | Enthalpic recuperator | 177.7 | 42.72 | 135 | 0 | 0.2404 |


https://doi.org/10.52202/077185-0012

| | | | | | | |
|---|---|---|---|---|---|---|
| 5 | Deareator | 755.3 | 580.4 | 174.8 | 0 | 0.7685 |
| 6 | Feedwater pump | 133.9 | 118.2 | 15.7 | 0 | 0.8827 |
| 7 | Biomass boiler | 48931 | 16775 | 32156 | 0 | 0.3428 |
| 8 | Solar field | - | - | - | - | - |
| 9 | Three-way valve | 1023 | 1019 | 4.135 | 0 | 0.996 |
| 10 | Dry cooler | 1019 | 90.74 | 0 | 928.1 | 0.08906 |

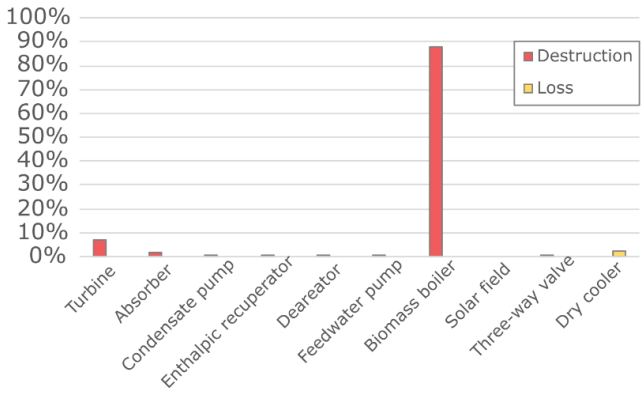


**Figure 2:** Contributions to exergy destruction and loss at $T_0$=35ºC and $\dot{Q}_{SOLAR}$=0.

### 3.2 Influence of ambient temperature and solar irradiation

After evaluating the potential of the cycle configuration for working effectively under high ambient temperatures, the results of the parametric analysis for different ambient temperatures and solar power values and their effects on the cycle performance are presented. Firstly, the introduction of solar power to the reference case will be commented. When 5 MW of solar thermal power are introduced into the cycle with the same ambient temperature of 35ºC, the most appreciable change from the viewpoint of energy analysis is the decrease of the required thermal power from the biomass combustion, that drops down to 32.975 MW. As liquid water is diverted from the steam drum to absorb the solar thermal power and then reinjected into it, no changes in the rest of thermodynamic states of the cycle are observed. Therefore, the energy efficiency of the cycle, defined as the net power obtained per unit heating power supplied to the cycle, is fixed at 32.31%.

Nevertheless, the reorganization of the heating flows in the cycle shifts the results of the exergy analysis, as collected in Table 4. First of all, a reduction in the exergy efficiency of the biomass boiler is observed, from 34.28% to 34.10%. However, thanks to the coupling to the solar field, with an exergy efficiency of 64.82%, the cycle is able to increase its exergy efficiency from 25.43% to 27.03%, suggesting a better utilization by the cycle of the heat input.

**Table 4:** Exergy analysis at $T_0$=35ºC with 5 MW added solar thermal power.

| ID | Component | $\dot{E}x_F$ [kW] | $\dot{E}x_P$ [kW] | $\dot{E}x_D$ [kW] | $\dot{E}x_L$ [kW] | $\varepsilon$ [-] |
|---|---|---|---|---|---|---|
| 1 | Turbine | 15097 | 12500 | 2597 | 0 | 0.828 |
| 2 | Absorber | 1602 | 966.1 | 635.9 | 0 | 0.6031 |
| 3 | Condensate pump | 94.41 | 81.07 | 13.34 | 0 | 0.8587 |
| 4 | Enthalpic recuperator | 177.7 | 42.72 | 135 | 0 | 0.2404 |
| 5 | Deareator | 755.3 | 580.4 | 174.8 | 0 | 0.7685 |
| 6 | Feedwater pump | 133.9 | 118.2 | 15.7 | 0 | 0.8827 |
| 7 | Biomass boiler | 42489 | 14487 | 28002 | 0 | 0.341 |
| 8 | Solar field | 3530 | 2288 | 1242 | 0 | 0.6482 |
| 9 | Three-way valve | 1023 | 1019 | 4.135 | 0 | 0.996 |
| 10 | Dry cooler | 1019 | 90.74 | 0 | 928.1 | 0.08906 |



https://doi.org/10.52202/077185-0012

When observing the contributions of cycle equipment to total exergy destruction and exergy loss, represented in Figure 3, the biomass boiler is again the component with the highest contribution to exergy destruction, but decreasing to around 83%. The turbine increases its contribution to 7.7%, and the solar field contributes with 3.68%. Again, the net contribution to destruction and losses of the rest of equipment is not so significant. Based on the previous results, the introduction of the solar field in parallel to the evaporator circuit of the biomass boiler reduces the amount of biomass burnt and helps to increase the exergy efficiency of the cycle but leaves the rest of the cycle unaffected. For new power plants, a solar field coupled to a heat storage technology could represent a better alternative in terms of exergy efficiency.

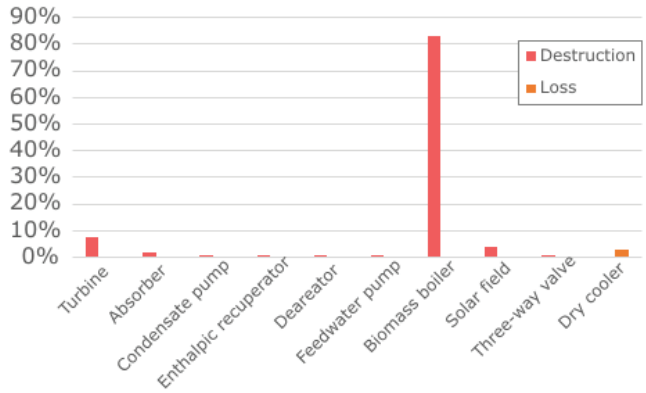


**Figure 3:** Contributions to exergy destructions and losses at $T_0$=35ºC and $\dot{Q}_{SOLAR}$ = 5 MW.

After analyzing this reference case, a parametric analysis with temperatures from 5ºC to 50ºC and solar thermal power values from 0 to 5 MW was performed. Some results were found to depend only on the ambient temperature, while others depended on the solar thermal power and others showed a dependence on both factors.

Considering the influence of ambient temperature, it affects the thermal energy dissipation process at the dry cooler through its operating temperatures. As the condensing pressure was modified according to this temperature to optimize the cycle, it led to small changes in the cycle mass flowrates. The feeding pump power was almost independent of both ambient temperature and solar thermal power, increasing slightly from 133.1 to 140 kW in the ambient temperature range between 5ºC and 50ºC. The work of the condensate pump, on the other hand, decreased from 145.5 to 85.7 kW, thanks to the adjustment of the temperature drop in the dry coolers. Nevertheless, the net power of the cycle remains almost constant, with values around 12.27 MW for all ambient conditions. It has been observed that the amount of thermal power that the cycle requires decreases as the temperature is lowered, reaching a minimum of 35.372 MW at 15ºC and becoming constant afterwards. This results in the values of cycle efficiency plotted in Figure 4, which show a decreasing trend with temperature, but reaching still competitive values at high ambient temperatures (30.52% at 50ºC ambient temperature). Therefore, this cycle configuration may prove useful in hot and dry climate conditions. Note that, as shown in Figure 5, the amount of biomass to be burnt increases with ambient temperature, in order to be able to supply the same net power to the grid.

When solar thermal power is introduced to the cycle, a reduction in the biomass consumption is observed, as shown in Figure 5. An average of 0.31 kg/s of biomass may be saved if 5 MW of solar thermal power are introduced into the cycle. Considering that hot and dry climate conditions are usually correlated with high solar irradiance values, the drop in the energy efficiency of the cycle may be compensated with the introduction of the solar field and the reduction in biomass consumption.


https://doi.org/10.52202/077185-0012

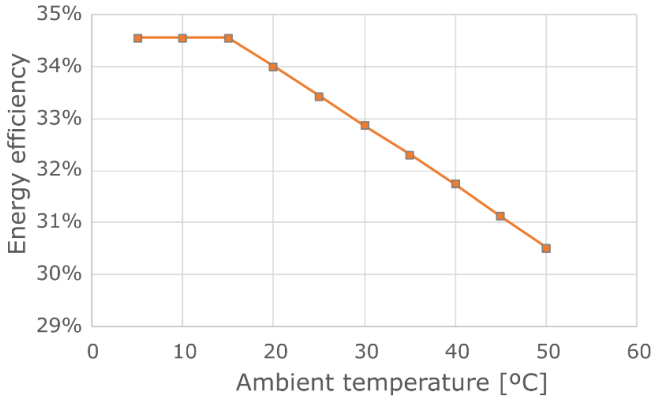


**Figure 4:** Cycle energy efficiency as a function of ambient temperature.

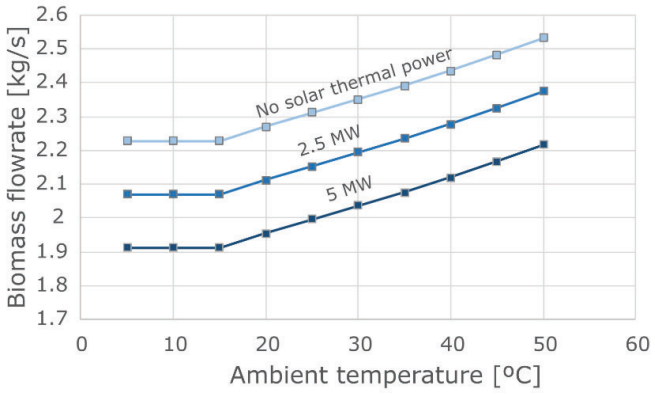


**Figure 5:** Biomass consumption as a function of ambient temperature.

The exergy efficiency, as depicted in Figure 6, depends on both ambient temperature and solar thermal power integration. The ambient temperature causes a similar effect as for the energy efficiency, with a decreasing trend starting at 15ºC. Exergy efficiency passes from a maximum around 29% at 5ºC and 5 MW of solar thermal power to a minimum of around 24% at 50ºC and no solar thermal power. In general, the increase in solar thermal power shifts the exergy efficiency curves upwards by around 1.7% when 5 MW of solar thermal power are introduced. Therefore, considering the best possible use of energy, maximization of solar thermal power should be the preferred option.

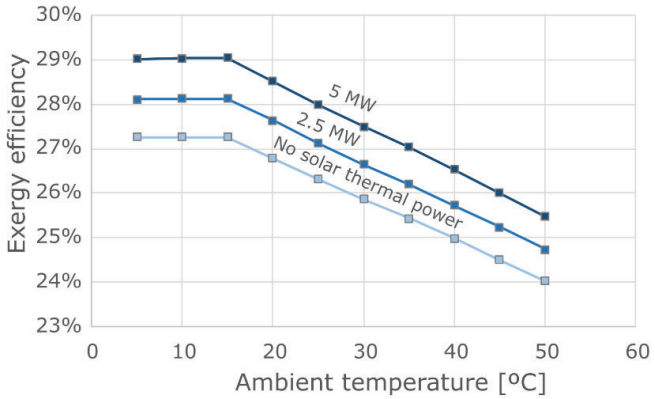


**Figure 6:** Cycle exergy efficiency as a function of ambient temperature and solar thermal power.



https://doi.org/10.52202/077185-0012

For the specific case of this study, as biomass is a byproduct of olive oil production, it does not need to be bought by the company; hence, reducing the amount of biomass burnt does not translate directly into an economic benefit. However, part of the olive oil production residue could be used for other purposes (i.e. fertilizers) instead of for powering the cycle boiler, reducing indeed the carbon and sulfur dioxide emissions from the power plant. As the reduction of the amount of biomass burnt depends only on the amount of integrated solar power, Equations 21 and 22 have allowed to generate Figure 7, which depicts the reduction in carbon dioxide (in tons per day) and sulfur dioxide (in kg per day) as a function of the integrated solar thermal power. For instance, integrating 5 MW of solar power results in decreasing the biomass burnt in 0.315, resulting in the avoidance of 16.637 tons of $CO_2$ and 25.4 kg of $SO_2$ per day.

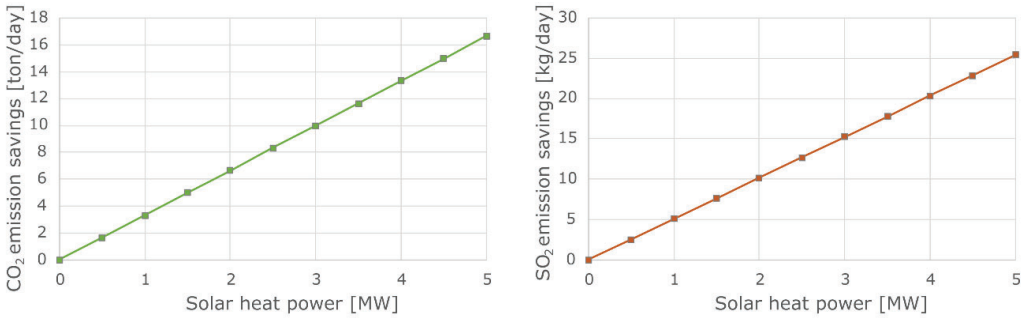


**Figure 7:** Carbon and sulfur dioxide emissions avoided as a function of solar thermal power.

## 4 CONCLUSIONS

A proposal for the integration of a solar field in an existing 12.5 MW biomass cycle incorporating the Hygroscopic Cycle Technology and using orujillo, a byproduct of olive oil production, as fuel has been analyzed in this work. Energy and exergy analyses have been conducted, and a rough estimate of the avoided carbon and sulfur dioxide emissions thanks to the integration of solar power has been provided.

The original cycle has shown to be able to work effectively at 35ºC ambient temperature with energy and exergy efficiency values of 32.31% and 25.43%. The configuration of the cycle allows heat rejection to the environment thanks to the use of dry coolers up to ambient temperatures of 50ºC thanks to the control of the condensing pressure. Therefore, the technology seems promising for the predicted scenarios of water scarcity and rising ambient temperatures. The results from the exergy analysis showed that the biomass boiler is the component with the highest contribution to exergy destruction.

Ambient temperature was found to influence heat dissipation at the dry cooler, requiring higher condensing pressures to be able to release heat to the environment and keep the net power of the cycle around a constant value of 12.27 MW. The cycle was found to keep competitive energy efficiency values up to an ambient temperature of 50ºC. Therefore, this cycle configuration may prove useful in hot and dry climate conditions.

Solar thermal power integration resulted in a noticeable increase in the exergy efficiency of the cycle, around 1.7% for the integration of 5 MW. In addition, the emission of 16.637 tons of $CO_2$ and 25.4 kg of $SO_2$ per day can be avoided with solar integration, encouraging the combination of biomass and solar energy as heat sources for the cycle. As this power plant runs on orujillo as fuel, with no direct cost to the olive oil company, an economic analysis considering yearly olive oil production and other uses for orujillo as a byproduct could provide information on the maximum amount of solar power that can be integrated without compromising the accumulation of orujillo as a residual waste.

Finally, the incorporation of the Hygroscopic Cycle Technology in power cycles seems promising in regions with water scarcity and high ambient temperatures. Considering that these regions tend to have higher solar irradiation values, the design of new power plants should consider solar power integration, even shifting to a 100% solar cycle coupled to heat storage technologies. The case study presented here


https://doi.org/10.52202/077185-0012

may be extrapolated to other Mediterranean locations with similar climate conditions as a solution for sustainable energy generation.

## NOMENCLATURE

| | | |
|---|---|---|
| DSG | Direct Steam Generation | |
| $\dot{E}x$ | Exergy flowrate | (kW) |
| $f_{dil}$ | dilution factor | (–) |
| h | specific enthalpy | (kJ/kg) |
| LHV | lower heating value | (kJ/kg) |
| $\dot{m}$ | mass flowrate | (kg/s) |
| PTC | Parabolic Trough Collectors | |
| $\dot{Q}$ | thermal power | (kW) |
| s | specific entropy | (kJ/(kg·K)) |
| T | temperature | (ºC, K) |
| $\dot{W}$ | power | (kW) |

**Symbols**

| | | |
|---|---|---|
| $\beta$ | exergy-heating value experimental coefficient | (–) |
| $\varepsilon$ | exergy efficiency of component | (–) |
| $\eta_b$ | boiler efficiency | (–) |
| $\eta_I$ | cycle energy efficiency | (–) |
| $\eta_{II}$ | cycle exergy efficiency | (–) |

**Subscript**

| | |
|---|---|
| 0 | ambient conditions |
| i | index of state i |
| ind | indirect |
| BIO | biomass |
| CP | condensate pump |
| D | destruction |
| DC | dry cooler |
| ECO | economizer |
| EVA | evaporator |
| FP | feedwater pump |
| L | loss |
| SH | superheater |

## REFERENCES

ANEO - Asociación Nacional de Empresas de Aceite de Orujo, 2024, *Biomasa*. https://www.aneorujo.es/biomasa/#orujillo (accessed in Feb 2024).

Axon, C.J, Darton, R.C., 2021, Sustainability and risk – a review of energy security, *Sustainable Production and Consumption*, vol. 27., pp. 1195-204.

F-Chart Software, *EES Engineering Equation Solver*. https://www.fchartsoftware.com/ees/ (accessed in Feb 2024).

Fiaschi, D., Manfrida, G., Mendecka, B., Tosti, L., Parisi, M.L., 2021, A Comparison of Different Approaches for Assessing Energy Outputs of Combined Heat and Power Geothermal Plants. *Sustainability*, vol.13, no.8, article 4527.

He, C., Liu, Z., Wu, J., Pan, X., Fang, Z., Li, J., Bryan, B. A, 2021, Future global urban water scarcity and potential solutions. *Nature Communications*, vol. 12, article 4667.

IEA (2023), *World Energy Outlook 2023*, IEA, Paris https://www.iea.org/reports/world-energy-outlook-2023 (accessed in Feb 2024).



https://doi.org/10.52202/077185-0012

Ke, X., Zhang, Y., Liu, X., Wu, Y., Huang, Z., Zhang, M. Lyu, J., Zhou, T., 2022, Development of biomass-fired circulating fluidized bed boiler with high steam parameters based on theoretical analysis and industrial practices, *J. of the Energy Institute*, vol. 105, p. 415-23.

Lazzaretto, A., Tsatsaronis, G., 2006, SPECO: A systematic and general methodology for calculating efficiencies and costs in thermal systems, *Energy*, vol. 31, no.8-9, p. 1257-89.

Nsanzubuhoro, C.N., Bello-Ochende, T., Malan, A.G., 2020, Second law analysis of a fossil-geothermal hybrid power plant with thermodynamic optimization of geothermal preheater, *Heat Transfer*, vol. 49, no. 7, pp. 3997–4018.

Rubio-Serrano, F.J., Gutiérrez-Trashorras, A.J., Soto-Pérez, F., Álvarez-Álvarez, E., Blanco-Marigorta, E., 2018, Advantages of incorporating Hygroscopic Cycle Technology to a 12.5-MW biomass power plant, *Applied Thermal Engineering*, vol. 131, p. 320-27.

Suárez-López, M.J, Prieto, J.I, Blanco, E., García, D., 2020, Tests of an Absorption Cooling Machine at the Gijón Solar Cooling Laboratory. *Energies*, vol. 13, no. 15, article 3962.

Szargut, J., Styrylska, T., 1964, Approximate evaluation of the exergy of fuels. Brennst. *Wärme Kraft,* vol. 16, no. 12, p. 589-596.

United Nations, 2023, *The United Nations World Water Development Report 2023: Partnerships and Cooperation for Water*. UNESCO, Paris. 210 p.

Winter, C. J., Sizmann, R. L., Vant-Hull, L. L., 2012. Solar power plants: fundamentals, technology, systems, economics. Springer Science & Business Media.

Zhang, Z., Duan, L., Wang, Z, Ren, Y., 2022, General performance evaluation method of integrated solar combined cycle (ISCC) system, *Energy*, vol. 204, article 122472.

## ACKNOWLEDGEMENT

This work has been supported by the project "Improvement of energy performance of the Hygroscopic Cycle for power production" (PID2019-108325RB-I00/AEI/10.13039/501100011033) from the Agencia Estatal de Investigación, Ministerio de Ciencia e Innovación, Spain and "Severo Ochoa" grant program for training in research and teaching of the Principality of Asturias – Spain (BP20-176). The authors also want to acknowledge the contribution of the company IMATECH (IMASA Technologies, S.L.U.), proprietary of the Hygroscopic Cycle Technology, as well as the support from the University Institute of Industrial Technology of Asturias (IUTA), financed by the City Council of Gijón, Spain.



https://doi.org/10.52202/077185-0012